Available online at www.sciencedirect.com
SCIENCE DIRECT®
ELSEVIER
International Journal of Solids and Structures 42 (2005) 5356–5376
INTERNATIONAL JOURNAL OF SOLIDS and STRUCTURES
www.elsevier.com/locate/ijsolstr

Transient waves in an inhomogeneous hollow infinite cylinder

Michael El-Raheb *

Applied Mechanics, AKT Mission Research Corporation, 23052 Alcalde Drive, Laguna Hills, CA 92653-1327, USA

Received 18 February 2005
Available online 29 March 2005

Abstract

Effects on transient waves of circumferential and radial inhomogeneity are studied in a plane-strain hollow cylinder. A periodic circumferential inhomogeneity modulating a constant value is analyzed adopting the Galerkin method where trial functions are chosen as the axisymmetric and asymmetric modes of the homogeneous cylinder. A periodic radial inhomogeneity is analyzed by dividing the cylinder into annular segments of constant width. A stepwise variation in modulus is assumed where modulus is constant over each segment. Adopting transfer matrices, continuity of state variables at interfaces of segments establishes the global dynamic equilibrium of the segmented cylinder. The static-dynamic superposition method is employed to solve for transient response.

Keywords: Wave propagation; Hollow cylinder; Inhomogeneous property

1. Introduction

Propagation of transient stress waves in human tissue during projectile penetration concerns medical researchers as overpressure from these waves may cause indirect trauma in human organs. As the projectile penetrates into tissue, it moves material by replacing it with its own volume. When tissue fails, it acts more like a fluid, lessening the amount of material being compressed by the moving projectile. In the radial direction, tissue is compressed by an expanding cross-section of the projectile's smoothly curved nose. This rapid expansion generates compressive waves symmetric about the projectile's axis that attenuate with distance. El-Raheb (2004) develops a model that approximates penetrated tissue as a homogeneous hollow finite

* Tel.: +1 626 796 5528; fax: +1 626 583 8834.
E-mail address: mertrident@earthlink.net

0020-7683/$ - see front matter
doi:10.1016/j.ijsolstr.2005.02.030

cylinder with inner radius that of the projectile and a sufficiently large outer radius to avoid interference from reflections at the outer boundary during the simulation time. A radial velocity is prescribed at the cylinder's inner boundary over the finite projectile length accounting for radial expansion from projectile axial motion.

This work evaluates the effect on propagation of material inhomogeneity that may result either from spatial variation in modulus or asymmetric radial tearing. Since real tissue inhomogeneity is complicated to model, the analysis to follow treats two uncoupled types of material inhomogeneity; circumferential or θ-inhomogeneity and radial or r-inhomogeneity. θ-inhomogeneity is asymmetric as modulus E varies periodically with angular coordinate θ but remains constant along the radial coordinate r. In this case both extensional and shear waves are excited. r-inhomogeneity is axisymmetric as E varies only along r but remains constant along θ. In this case only extensional waves are excited. In practice both θ and r inhomogeneities exist in tissue, nevertheless the two types are presently addressed separately for parametric evaluation of each type's effect avoiding the cross-coupling that may result if both were acting together. Since histories from the homogeneous finite cylinder model (El-Raheb, 2004) compared favorably with those from the homogeneous plane-strain model, the latter model is adopted for studying material inhomogeneity.

Whittier and Jones (1967) studied the propagation of longitudinal and torsional waves in a bi-material solid cylinder composed of an inner homogeneous core bonded to an outer homogeneous annular cylinder of different properties. Armenakas (1967), Reuter (1969), Armenakas and Keck (1970), studied flexural waves in bi-material cylinders. Keck and Armenakas (1971) presented an exact solution for longitudinal waves in an infinitely long composite hollow cylinder made of three different transversely isotropic layers. Vibrations of homogeneous hollow plane-strain cylinders was analyzed by Gazis (1958), Bird et al. (1960), and Baltrukonis (1960). The references above were restricted to three concentric axisymmetric layers. Yin and Yue (2002) analyzed the plain-strain axisymmetric problem with multiple annular layers using Laplace transforms to integrate time dependence. Heyliger and Jilania (1992) adopted a variational method and a Ritz approximation to study frequency response of inhomogeneous cylinders and spheres. Steinberg (1995) formulated the inverse spectral problem to determine properties of a cylinder with inhomogeneous materials. Inertial θ-inhomogeneity from point masses attached to the wall of a thin cylinder was analyzed by El-Raheb and Wagner (1989).

In Section 2, θ-inhomogeneity is treated adopting the Galerkin method. Eigenfunctions of the asymmetric homogeneous dynamic equations are utilized as trial functions in the inhomogeneous dynamic equations. Orthogonality of radial and circumferential dependence produces an eigenvalue problem with coupling coefficients as the eigenvector. The static-dynamic superposition method is adopted to solve the transient response. In Section 3, a stepwise r-inhomogeneity is treated adopting transfer matrices of annular segments with varying properties. Continuity of stress and displacement at interfaces of segments yields a global transfer matrix producing eigenstates of the multi-layered cylinder. Once more, transient response is found adopting the static-dynamic superposition method. Section 4 discusses transient histories in hollow cylinders with the two types of inhomogeneity.

2. Circumferential inhomogeneity

Consider the plane-strain dynamic equilibrium equations in cylindrical coordinates

$$\begin{aligned} &\partial_r\sigma_{rr} + (\sigma_{rr} - \sigma_{\theta\theta})/r + 1/r\partial_\theta\tau_{r\theta} = \rho\partial_{tt}u \\ &\partial_r\tau_{r\theta} + 2\tau_{r\theta}/r + 1/r\partial_\theta\sigma_{\theta\theta} = \rho\partial_{tt}v \\ &r_p \leqslant r \leqslant r_o, \quad 0 \leqslant \theta \leqslant 2\pi \end{aligned} \tag{1a}$$

with boundary conditions

$$\begin{aligned}&\sigma_{rr}(r_p,\theta;t)=p_0 f_p(t),\quad \tau_{r\theta}(r_p,\theta;t)=0\\&\sigma_{rr}(r_o,\theta;t)=0,\quad \tau_{r\theta}(r_o,\theta;t)=0\end{aligned}\tag{1b}$$

r_p and r_o are cylinder inner and outer radii, σ_{rr}, $\sigma_{\theta\theta}$, $\tau_{r\theta}$ are normal and shear stresses, (r,θ) are radial and circumferential coordinates, (u,v) are corresponding displacements, ρ is density, t is time, p_0 is magnitude of uniform pressure applied at $r=r_p$ and $f_p(t)$ is its time dependence. The constitutive relations are

$$\begin{aligned}&\sigma_{ii}=\lambda\Delta+2\mu\varepsilon_{ii},\quad ii\equiv rr,\ \theta\theta,\ zz\\&\Delta=\varepsilon_{rr}+\varepsilon_{\theta\theta},\quad \varepsilon_{zz}=0\\&\sigma_{ij}=\mu\varepsilon_{ij},\quad ij\equiv r\theta,\ \theta z,\ zr\end{aligned}\tag{2a}$$

$$\begin{aligned}&\varepsilon_{rr}=\partial_r u,\quad \varepsilon_{\theta\theta}=u/r+1/r\partial_\theta v,\quad \varepsilon_{zz}=0\\&\varepsilon_{r\theta}=1/r\partial_\theta u+\partial_r v-v/r\end{aligned}\tag{2b}$$

(λ,μ) are the *Lame*' constants. For the homogeneous medium, substituting (2b) in (2a) then in (1a) yields the dynamic displacement equations

$$\begin{aligned}&\mu(D_{11}u+D_{12}v)=\rho\partial_{tt}u\\&\mu(D_{21}u+D_{22}v)=\rho\partial_{tt}v\end{aligned}\tag{3}$$

$$D_{11}\equiv[(\beta+2)\hat{\nabla}_1^2+1/r^2\partial_{\theta\theta}],\quad D_{12}\equiv 1/r\partial_\theta[(\beta+1)\partial_r-(\beta+3)/r]$$

$$D_{21}\equiv 1/r\partial_\theta[(\beta+1)\partial_r+(\beta+3)/r],\quad D_{22}\equiv[\hat{\nabla}_1^2+(\beta+2)/r^2\partial_{\theta\theta}]$$

$$\hat{\nabla}_1^2\equiv\partial_{rr}+1/r\partial_r-1/r^2,\quad \beta=\lambda/\mu=2\nu/(1-2\nu)$$

ν is Poisson's ratio. Eq. (3) is the limiting case of Eq. (A.1) in Appendix A when the z dependence vanishes.

Assume a circumferentially inhomogeneous modulus $\mu(\theta)$ symmetric about $\theta=0$ with a Fourier expansion

$$\mu(\theta)=\mu_0\sum_{l=0}^{N_E}e_l C_l(\theta),\quad S_l(\theta)=\sin(l\theta),\quad C_l(\theta)=\cos(l\theta)\tag{4}$$

Substituting (4) in (2a,b) then in (1a) produces the equations

$$\sum_{l=0}e_l C_l(\theta)\mu_0(D_{11}u+D_{12}v)+\sum_{l=1}e_l l S_l(\theta)\mu_0(\widetilde{D}_{11}u+\widetilde{D}_{12}v)=\rho\partial_{tt}u\tag{5a}$$

$$\sum_{l=0}e_l C_l(\theta)\mu_0(D_{21}u+D_{22}v)+\sum_{l=1}e_l l S_l(\theta)\mu_0(\widetilde{D}_{21}u+\widetilde{D}_{22}v)=\rho\partial_{tt}v\tag{5b}$$

$$\widetilde{D}_{11}\equiv-1/r^2\partial_\theta,\quad \widetilde{D}_{12}\equiv-1/r\partial_r+1/r^2$$

$$\widetilde{D}_{21}\equiv-\beta/r\partial_r-(\beta+2)/r^2,\quad \widetilde{D}_{22}\equiv-(\beta+2)/r^2\partial_\theta$$

To solve (5), the Galerkin method is adopted. u and v are expanded in terms of orthogonal trial functions satisfying the boundary conditions at the inner and outer walls of the cylinder $r=r_p$ and $r=r_o$. One admissible set is the eigenfunctions of the homogeneous problem in Eq. (3) with $\mu=\mu_0$ the axisymmetric term in the $\mu(\theta)$ expansion (4). For harmonic motions in time with radian frequency ω and periodicity along θ, the solution to (1a) is

$$u(r,\theta,t) = (u_1(r,\theta) + u_2(r,\theta))e^{i\omega t}$$
$$\upsilon(r,\theta,t) = (\upsilon_1(r,\theta) + \upsilon_2(r,\theta))e^{i\omega t} \tag{6a}$$

$$u_1 = \sum_{n=0}\{c_{11n}k_{re}(nJ_n(k_{re}r)/(k_{re}r) - J_{n+1}(k_{re}r)) + c_{12n}nJ_n(k_{rs}r)/r\}C_n(\theta)$$
$$\upsilon_1 = \sum_{n=0}\{-c_{11n}nJ_n(k_{re}r)/r - c_{12n}k_{rs}(nJ_n(k_{rs}r)/(k_{rs}r) - J_{n+1}(k_{rs}r))\}S_n(\theta) \tag{6b}$$
$$S_n(\theta) = \sin(n\theta), \quad C_n(\theta) = \cos(n\theta)$$

(u_1, υ_1) are derived in Eqs. (B.1) of Appendix B, and (u_2, υ_2) have the same form as (u_1, υ_1) with $J_n(kr)$ replaced by $Y_n(kr)$ and (c_{21n}, c_{22n}) replacing (c_{11n}, c_{12n}). Expressions for σ_{rr}, $\tau_{r\theta}$ similar to those for displacement in (6a) and (6b) can be expressed as

$$\sigma_{rr}(r,\theta,t) = (\sigma_{rr1}(r,\theta) + \sigma_{rr2}(r,\theta))e^{i\omega t}$$
$$\tau_{r\theta}(r,\theta,t) = (\tau_{r\theta1}(r,\theta) + \tau_{r\theta2}(r,\theta))e^{i\omega t} \tag{7a}$$

$$\sigma_{rr1} = \mu\sum_{n=0}\{c_{11n}((-(\beta+2)(k_{re}r)^2 + 2(n^2-n))J_n(k_{re}r)/r^2 + 2k_{re}J_{n+1}(k_{re}r)/r) + 2c_{12n}((n^2-n)J_n(k_{rs}r)/r^2 - nk_{rs}J_{n+1}(k_{rs}r)/r)\}C_n(\theta) \tag{7b}$$

$$\tau_{r\theta1} = \mu\sum_{n=0}\{2c_{11n}(-(n^2-n)J_n(k_{re}r)/r^2 + nk_{re}J_{n+1}(k_{re}r)/r) - 2c_{12n}((n^2-n-(k_{rs}r)^2/2)J_n(k_{rs}r)/r^2 + k_{rs}J_{n+1}(k_{rs}r)/r)S_n(\theta) \tag{7c}$$

$(\sigma_{rr1}, \tau_{r\theta1})$ are derived in Eqs. (B.2) of Appendix B, (k_{re}, k_{rs}) are radial wave numbers defined in Eqs. (B.1) of Appendix B. $(\sigma_{rr2}, \tau_{r\theta2})$ have the same form as $(\sigma_{rr1}, \tau_{r\theta1})$ with $J_n(kr)$ replaced by $Y_n(kr)$ and (c_{11n}, c_{12n}) replaced by (c_{21n}, c_{22n}). Re-write (7a) in the form

$$\mathbf{S}(r,\theta,t) \equiv \{\sigma_{rr}, \tau_{r\theta}\}^{\mathrm{T}} = \sum_{n=0}\boldsymbol{\vartheta}_n(\theta)\overline{\mathbf{B}}_n(r)c_n e^{i\omega t}$$
$$\vartheta_n(\theta) = \begin{vmatrix} C_n(\theta) & 0 \\ 0 & S_n(\theta) \end{vmatrix} \tag{8}$$

$\overline{\mathbf{B}}_n(r)$ is a 2×4 matrix of the radial functions in $(\sigma_{rr}, \tau_{r\theta})$ multiplying $\mathbf{c}_n = \{c_{11n}, c_{12n}, c_{21n}, c_{22n}\}^{\mathrm{T}}$ in (7b,c). The homogeneous boundary conditions (1a) are

$$\sigma_{rr}(r_p) = 0, \quad \sigma_{rr}(r_o) = 0 \tag{9a}$$

$$\tau_{r\theta}(r_p) = 0, \quad \tau_{r\theta}(r_o) = 0 \tag{9b}$$

Substituting (8) in (9a,b) and enforcing orthogonality of the θ dependence yields a set of uncoupled eigenvalue problems for each circumferential wave number n

$$\mathbf{B}_n\mathbf{c}_n = \mathbf{0}, \quad \mathbf{B}_n = \begin{bmatrix} \overline{\mathbf{B}}_n(r_p) \\ \overline{\mathbf{B}}_n(r_o) \end{bmatrix}$$
$$\Rightarrow \det|\mathbf{B}_n| = 0 \Rightarrow \{\varphi(r), \psi(r); \omega\}_{mn} \tag{10}$$

$\mathbf{B}_n$ is a 4×4 matrix, $\{\varphi(r), \psi(r)\}_{mn}$ are the displacement eigenfunctions, ω_{mn} are the eigenvalues, and m is radial wave number. In what follows $\varphi_{mn}(r)$ and $\psi_{mn}(r)$ will be written as φ_{mn} and ψ_{mn} for shortness since it is known that they are functions of r only. Expand (u, υ) in the eigenfunctions (9)

$$u(r,\theta,t)=\sum_{n=0}\sum_{m=1}a_{mn}(t)\varphi_{mn}C_n(\theta)$$
$$\upsilon(r,\theta,t)=\sum_{n=1}\sum_{m=1}a_{mn}(t)\psi_{mn}S_n(\theta) \tag{11}$$

Substituting (11) in (5a,b) yields

$$\mu_0\sum_{l=0}e_lC_l(\theta)\sum_{k=0}\sum_{j=1}a_{jk}(t)(D_{11}^{(r)}\varphi+D_{12}^{(r)}\psi)_{jk}C_k(\theta)+\mu_0\sum_{l=1}e_llS_l(\theta)\sum_{k=1}\sum_{j=1}a_{jk}(t)(\widetilde{D}_{11}^{(r)}\varphi+\widetilde{D}_{12}^{(r)}\psi)_{jk}S_k(\theta)$$
$$=\rho\sum_{n=0}\sum_{m=1}\ddot{a}_{mn}(t)\varphi_{mn}C_n(\theta)$$
$$S_k(\theta)=\sin(k\theta),\quad C_k(\theta)=\cos(k\theta) \tag{12a}$$

$$\mu_0\sum_{l=0}e_lC_l(\theta)\sum_{k=1}\sum_{j=1}a_{jk}(t)(D_{21}^{(r)}\varphi+D_{22}^{(r)}\psi)_{jk}S_k(\theta)+\mu_0\sum_{l=1}e_llS_l(\theta)\sum_{k=0}\sum_{j=1}a_{jk}(t)(\widetilde{D}_{21}^{(r)}\varphi+\widetilde{D}_{22}^{(r)}\psi)_{jk}C_k(\theta)\rho$$
$$=\rho\sum_{n=1}\sum_{m=1}\ddot{a}_{mn}(t)\psi_{mn}S_n(\theta) \tag{12b}$$

In (12a,b) the operators $D_{ij}^{(r)}$ are the same as D_{ij} in (5) with the θ dependence eliminated, and $(\bullet)$ is derivative with respect to t. From Eq. (3), noting that

$$(D_{11}^{(r)}\varphi+D_{12}^{(r)}\psi)_{jk}=-\rho/\mu_0\omega_{jk}^2\varphi_{jk}$$
$$(D_{21}^{(r)}\varphi+D_{22}^{(r)}\psi)_{jk}=-\rho/\mu_0\omega_{jk}^2\psi_{jk} \tag{13}$$

reduces (12) to

$$-\sum_{l=0}e_lC_l(\theta)\sum_{k=0}\sum_{j=1}\omega_{jk}^2a_{jk}(t)\varphi_{jk}C_k(\theta)-\mu_0\Big/\rho\sum_{l=1}e_llS_l(\theta)\sum_{k=1}\sum_{j=1}a_{jk}(t)(-n\varphi_{jk}/r^2-\psi_{jk}/r^2+\psi'_{jk}/r)S_k(\theta)$$
$$=\sum_{n=0}\sum_{m=1}\ddot{a}_{mn}(t)\varphi_{mn}C_n(\theta) \tag{14a}$$

$$-\sum_{l=0}e_lC_l(\theta)\sum_{k=1}\sum_{j=1}\omega_{jk}^2a_{jk}(t)\psi_{jk}S_k(\theta)-\mu_0\Big/\rho\sum_{l=1}e_llS_l(\theta)\sum_{k=0}\sum_{j=1}a_{jk}(t)(\beta\varphi'_{jk}/r$$
$$+(\beta+2)\varphi_{jk}/r^2+n(\beta+2)\psi_{jk}/r^2)C_k(\theta)$$
$$=\sum_{n=1}\sum_{m=1}\ddot{a}_{mn}(t)\psi_{mn}S_n(\theta) \tag{14b}$$

For each (m,n) dyad, multiplying both sides of Eq. (14a) by $\varphi_{mn}\cos(n\theta)$ and both sides of (14b) by $\psi_{mn}\sin(n\theta)$, integrating over the domain $r_p\leqslant r\leqslant r_o$, $0\leqslant\theta\leqslant 2\pi$ then adding the two resulting equations produces

$$(1+\delta_{n0})\pi N_{mn}\ddot{a}_{mn}(t)+\sum_{k=0}\sum_{j=1}\left[\Theta_{nk}^{(1)}R_{mn,jk}^{(1)}+\Theta_{nk}^{(2)}R_{mn,jk}^{(2)}\right]\omega_{jk}^2a_{jk}(t)$$
$$+\mu_0\Big/\rho\sum_{k=0}\sum_{j=1}\left[\Theta_{nk}^{(3)}R_{mn,jk}^{(3)}+\Theta_{nk}^{(4)}R_{mn,jk}^{(4)}\right]a_{jk}(t)=0 \tag{15a}$$

$$N_{mn}=\int_{r_p}^{r_o}(\varphi_{mn}^2+\psi_{mn}^2)r\,\mathrm{d}r,\quad n=0,1,\ldots,N_\theta,\ m=1,2,\ldots,N_r$$

$$\Theta^{(1)}_{nk} = \sum_{l=0} e_l \int_0^{2\pi} C_l(\theta)C_k(\theta)C_n(\theta)\,\mathrm{d}\theta, \quad \Theta^{(2)}_{nk} = \sum_{l=0} e_l \int_0^{2\pi} C_l(\theta)S_k(\theta)S_n(\theta)\,\mathrm{d}\theta$$
$$\Theta^{(3)}_{nk} = \sum_{l=1} e_l l \int_0^{2\pi} S_l(\theta)S_k(\theta)C_n(\theta)\,\mathrm{d}\theta, \quad \Theta^{(4)}_{nk} = \sum_{l=1} e_l l \int_0^{2\pi} S_l(\theta)C_k(\theta)S_n(\theta)\,\mathrm{d}\theta \tag{15b}$$

$$R^{(1)}_{mn,jk} = \int_{r_p}^{r_o} \varphi_{mn}\varphi_{jk} r\,\mathrm{d}r, \quad R^{(2)}_{mn,jk} = \int_{r_p}^{r_o} \psi_{mn}\psi_{jk} r\,\mathrm{d}r$$
$$R^{(3)}_{mn,jk} = \int_{r_p}^{r_o} \varphi_{mn}(-k\varphi_{jk}/r^2 - \psi_{jk}/r^2 + \psi'_{jk}/r) r\,\mathrm{d}r \tag{15c}$$
$$R^{(4)}_{mn,jk} = \int_{r_p}^{r_o} \psi_{mn}(\beta\varphi'_{jk}/r + (\beta+2)\varphi_{jk}/r^2 + k(\beta+2)\psi_{jk}/r^2) r\,\mathrm{d}r$$

δ_{n0} is the Kronecker delta and $(\ )'$ is derivative w.r.t. r. In arriving at (14a) the orthogonality of $(\varphi_{mn}, \psi_{m\,n})$ was utilized. For a homogeneous material, $\Theta^{(3)}_{nk} = \Theta^{(4)}_{nk} = 0$, $\Theta^{(1)}_{nk} = \Theta^{(2)}_{nk} = (1+\delta_{n0})\pi$ and $R^{(1)}_{mn,jk} + R^{(2)}_{mn,jk} = N_{mn}\delta_{mj}\delta_{nk}$ reducing (11a) to the simple form

$$\ddot{a}_{mn}(t) + \omega^2_{mn} a_{mn}(t) = 0 \tag{16}$$

To diagonalize (14a,b), form the coupled eigenproblem

$$[\mathbf{K}_c - \mathbf{M}_c\omega_c^2]\mathbf{a} = \mathbf{0}, \quad \mathbf{a} = \{a_{mn}\}^{\mathrm{T}}$$
$$K_{c\,mn,jk} = \omega^2_{jk}[\Theta^{(1)}_{nk} R^{(2)}_{mn,jk} + \Theta^{(2)}_{nk} R^{(2)}_{mn,jk}] + \mu_0/\rho[\Theta^{(3)}_{nk} R^{(3)}_{mn,jk} + \Theta^{(4)}_{nk} R^{(4)}_{mn,jk}] \tag{17}$$
$$M_{c\,mn,jk} = (1+\delta_{n0})\pi N_{mn}\delta_{mj}\delta_{nk}$$

$\mathbf{K}_c$ is a stiffness matrix of order $(N_r N_\theta)\times(N_r N_\theta)$, $\mathbf{M}_c$ is a diagonal mass matrix of the same order. The eigenproblem (13) yields the orthogonal eigenset $\{\Phi_{ci}(r,\theta);\ \omega_{ci}\}$ where $\Phi_{ci}(r,\theta)$ is the ith eigenvector coupling the constituent modes $\{\varphi_{mn}, \psi_{mn}\}$ by the coupling coefficients $\{a_{mn,i}\}^{\mathrm{T}}$, and ω_{ci} are the corresponding eigen-frequencies. The coupled state vector $\mathbf{S}_c = \{u_c, \upsilon_c, \sigma_{rrc}, \sigma_{\theta\theta c}, \sigma_{zzc}, \tau_{r\theta c}\}^{\mathrm{T}}$ can be expanded in terms of $\Phi_{ci}(r,\theta)$ as

$$\mathbf{S}_c(r,\theta;t) = \sum_i c_i(t)\Phi_{ci}(r,\theta) \tag{18a}$$

$$\Phi_{cl}(r,\theta) = \sum_n \sum_m a_{mn,l} S_{mn}(r,\theta)$$
$$\Phi_{ci}(r,\theta) = \{\bar{u}_c, \bar{\upsilon}_c, \bar{\sigma}_{rrc}, \bar{\sigma}_{\theta\theta c}, \bar{\sigma}_{zzc}, \bar{\tau}_{r\theta c}\}^{\mathrm{T}}_i \tag{18b}$$

$\mathbf{S}_{mn}$ is the state eigenvector of the (m,n)th constituent mode and $\bar{u}_{ci}, \bar{\upsilon}_{ci}, \ldots, \bar{\tau}_{r\theta ci}$ are components of the ith coupled eigenvector $\mathbf{\Phi}_{ci}(r,\theta)$.

Express displacement $\mathbf{u}(r,\theta;t)$ as a superposition of two terms

$$\mathbf{u}(r,\theta;t) = \mathbf{u}_s(r,\theta) f_p(t) + \mathbf{u}_d(r,\theta;t) \tag{19}$$

$\mathbf{u}_s(r,\theta)$ is static displacement vector satisfying (5) with vanishing time dependence and boundary conditions (1b) with $f_p(t) = 1$ (see Appendix C), $\mathbf{u}_d(r,\theta;t)$ is dynamic displacement vector satisfying (5) and boundary conditions (1b) with $f_p(t) = 0$

$$u_s(r,\theta) = u_{s0}(r) + \sum_{n=0} U_{sn} C_n(\theta), \quad \upsilon_s(r,\theta) = \sum_{n=0} V_{sn} S_n(\theta)$$
$$U_{sn} = \sum_{m=1} b_{mn}\varphi_{mn}, \quad V_{sn} = \sum_{m=1} b_{mn}\psi_{mn} \tag{20}$$

$u_{s0}(r)$ is the axisymmetric radial displacement satisfying the inhomogeneous boundary condition (1b) with $f_p(t) = 1$ (see Appendix C). Expand $\mathbf{u}_d(r,\theta;t)$ in the eigenfunctions $(\bar{u}_{ci}, \bar{v}_{ci})$

$$\begin{aligned} u_d(r,\theta;t) &= \sum_i c_i(t)\bar{u}_{ci}(r,\theta), \quad \bar{u}_{ci}(r,\theta) = \sum_{n=0}\sum_{m=1} a_{mn,i}\varphi_{mn}C_n(\theta) \\ v_d(r,\theta;t) &= \sum_i c_i(t)\bar{v}_{ci}(r,\theta), \quad \bar{v}_{ci}(r,\theta) = \sum_{n=1}\sum_{m=1} a_{mn,i}\psi_{mn}S_n(\theta) \end{aligned} \tag{21}$$

$c_i(t)$ is generalized coordinate of the ith coupled eigenfunction. Substituting (19)–(21) in (5) and enforcing orthogonality of the $\{\bar{u}_{ci}, \bar{v}_{ci}\}$ set yields uncoupled equations in $c_i(t)$

$$\ddot{c}_i(t) + \omega_{ci}^2 c_i(t) = \bar{f}_i(t) \tag{22a}$$

$$\begin{aligned} \bar{f}_i(t) &= N_{si}\ddot{f}_p(t)/N_{ii} \\ N_{ii} &= \int_0^{2\pi}\int_{r_p}^{r_o} (\bar{u}_{ci}^2 + \bar{v}_{ci}^2) r\,\mathrm{d}r\,\mathrm{d}\theta = \pi\sum_{n=0}(1+\delta_{n0})\int_{r_p}^{r_o}(U_{n,i}^2 + V_{n,i}^2) r\,\mathrm{d}r \\ N_{si} &= \int_0^{2\pi}\int_{r_p}^{r_o} (\bar{u}_{ci}u_s + \bar{v}_{ci}v_s) r\,\mathrm{d}r\,\mathrm{d}\theta \\ &= 2\pi\int_{r_p}^{r_o}(U_{s0} + u_{s0})U_{0,i} r\,\mathrm{d}r + \pi\sum_{n=1}\int_{r_p}^{r_o}(U_{n,i}U_{sn} + V_{n,i}V_{sn}) r\,\mathrm{d}r \\ U_{n,i} &= \sum_{m=1} a_{mn,i}\varphi_{mn}, \quad V_{n,i} = \sum_{m=1} a_{mn,i}\psi_{mn} \end{aligned} \tag{22b}$$

b_{mn} are coupling coefficients of the coupled static solution. Eq. (22a) admits the solution

$$c_i(t) = -\frac{1}{\omega_{ci}}\int_0^t \sin\omega_{ci}(t-\tau)\bar{f}_i(\tau)\,\mathrm{d}\tau \tag{23a}$$

If $f_p(t)$ is piecewise linear with n_s conjoined segments

$$\begin{aligned} f_p(t) &= \sum_{j=1}^{n_s}(\alpha_j + \beta_j(t-t_j))[H(t-t_j) - H(t-t_{j+1})] \\ \beta_j &= (f_p(t_{j+1}) - f_p(t_j))/(t_{j+1} - t_j), \quad \alpha_j = f_p(t_j), \quad t_1 = f_p(t_1) = 0 \\ \ddot{f}_p(t) &= \beta_1\delta(t) - \beta_{n_s}\delta(t - t_{n_s+1}) + \sum_{j=1}^{n_s-1}(\beta_{j+1} - \beta_j)\delta(t - t_{j+1}) \end{aligned} \tag{23b}$$

then (23a) can be integrated analytically with an accuracy independent of the time interval.

3. Radial inhomogeneity

Consider a stepwise radial variation in modulus as follows. Divide the region $r_p \leqslant r \leqslant r_o$ into N_r equidistant annular segments

$$\begin{aligned} &r_j \leqslant r \leqslant r_{j+1}, \quad j = 1,\ldots,N_r \\ &\Delta r = \Delta r_j = r_{j+1} - r_j = (r_o - r_p)/N_r \end{aligned} \tag{24}$$

Assume that $\mathbf{c}_j = \{c_{1j}, c_{2j}\}^{\mathrm{T}}$ is constant over each segment but varies from segment to segment. Since axial symmetry holds, the following equation applies to the jth segment

$$(\lambda+2\mu)_j(\partial_{rr}+1/r\partial_r-1/r^2)u_j=\rho\partial_{tt}u_j \tag{25}$$

For harmonic motions in time with radian frequency ω, Eq. (25) admits the solution for the jth segment

$$\begin{aligned} &u_j(r,t)=\bar{u}_j(r)e^{i\omega t}, \quad \bar{u}_j(r)=c_{1j}J_1(k_{ej}r)+c_{2j}Y_1(k_{ej}r)\\ &k_{ej}=\omega/c_{ej}, \quad c_{ej}^2=(\lambda+2\mu)_j/\rho \end{aligned} \tag{26}$$

Substituting (26) in the constitutive relations (2a,b) yields

$$\bar{\sigma}_{rrj}=\mu_j c_{1j}(-(\beta+2)k_{ej}J_0(k_{ej}r)+2J_1(k_{ej}r)/r)+\mu_j c_{2j}(-(\beta+2)k_{ej}Y_0(k_{ej}r)+2Y_1(k_{ej}r)/r) \tag{27}$$

For each annular segment, express the state vector $\mathbf{S}_j=\{\bar{\sigma}_{rrj},\bar{u}_j\}^{\mathrm{T}}$ in terms of the constant vector $\mathbf{c}_j=\{c_{1j},c_{2j}\}^{\mathrm{T}}$

$$\mathbf{S}_j(r)=\mathbf{B}_j(r)\mathbf{c}_j \tag{28}$$

$\mathbf{B}_j(r)$ is a matrix with coefficients the functions multiplying (c_{1j},c_{2j}) in (26) and (27). Evaluating (28) at the two ends of the jth segment then eliminating $\mathbf{c}_j$ determines the (2×2) transfer matrix $\mathbf{T}_j$ relating state vectors at the ends of a segment

$$\mathbf{S}_j(r_{j+1})=\mathbf{T}_j\mathbf{S}_j(r_j), \quad \mathbf{T}_j\equiv[t_{kl}^j]=\mathbf{B}_j^{-1}(r_j)\mathbf{B}_j(r_{j+1}) \tag{29a}$$

$$\mathbf{c}_j=\mathbf{B}_j^{-1}(r_j)\mathbf{S}_j(r_j) \tag{29b}$$

Enforcing continuity of $\mathbf{S}_j$ at interfaces of segments and homogeneous boundary conditions (8a) at $r=r_p$ and $r=r_o$ yields the global transfer matrix $\mathbf{T}_G$ in tri-diagonal block form and global $\mathbf{S}_G$ which is the ensemble of all $\mathbf{S}_j$

$$\begin{aligned} &\mathbf{T}_G\cdot\mathbf{S}_G=\mathbf{0} \;\Rightarrow\; \det|\mathbf{T}_G|=0\\ &\mathbf{S}_G=\{\mathbf{S}_1(r_1),\mathbf{S}_2(r_2),\ldots,\mathbf{S}_j(r_j),\ldots,\mathbf{S}_{N_r}(r_{N_r})\}^{\mathrm{T}} \end{aligned} \tag{30}$$

$$\mathbf{T}_G=\begin{bmatrix} -1 & 0 & & & & & & & & \\ t_{11}^1 & t_{12}^1 & -1 & 0 & & & & & & \\ t_{21}^1 & t_{22}^1 & 0 & -1 & & & & & & \\ & & t_{11}^2 & t_{12}^2 & -1 & 0 & & & & \\ & & t_{21}^2 & t_{22}^2 & 0 & -1 & & & & \\ & & & & \cdot & \cdot & & & & \\ & & & & \cdot & \cdot & t_{11}^{N_r} & t_{12}^{N_r} & -1 & 0 \\ & & & & & & t_{21}^{N_r} & t_{22}^{N_r} & 0 & -1 \\ & & & & & & & & -1 & 0 \end{bmatrix}$$

Eq. (30) determines the eigenset $\{\mathbf{S}_G;\omega\}$ and in turn $\mathbf{C}_j=\{\mathbf{c}_1,\mathbf{c}_2,\ldots,\mathbf{c}_j,\ldots,\mathbf{c}_{N_r}\}^{\mathrm{T}}$ from (29b).

To solve the transient response problem, decompose the displacement $u(r;t)$ as a superposition of two terms in the manner as was done for the circumferential inhomogeneity

$$u(r,t)=u_s(r)f_p(t)+u_d(r,t) \tag{31}$$

$u_s(r)$ is static displacement satisfying (25) with vanishing time dependence and boundary conditions (1b) with $f_p(t)=1$, and $u_d(r;t)$ is dynamic displacement satisfying (25) and boundary conditions (1b) with $f_p(t)=0$. The static state vector $\mathbf{S}_{sj}=\{\sigma_{rrs},u_s\}_j^{\mathrm{T}}$ of the jth segment takes the form

$$\sigma_{rrsj}(r)=2(\lambda+\mu)_j c_{1sj}+2\mu_j c_{2sj}/r^2 \tag{32a}$$

$$u_{sj}(r) = c_{1sj} r + c_{2sj}/r \tag{32b}$$

The global static transfer matrix is determined following the steps that led to Eqs. (28) and (29)

$$\begin{aligned} &\mathbf{T}_{Gs} \cdot \mathbf{S}_{Gs} = \mathbf{p}_0, \quad \mathbf{p}_0 = \{p_0, 0, 0, \ldots, 0\}^{\mathrm{T}} \\ &\mathbf{S}_{Gs} = \{\mathbf{S}_{s1}(r_1), \mathbf{S}_{s2}(r_2), \ldots, \mathbf{S}_{sj}(r_j), \ldots, \mathbf{S}_{sN_r}(r_{N_r})\}^{\mathrm{T}} \end{aligned} \tag{33}$$

Expand u_d in its eigenfunctions $\varphi_m(r)$

$$\begin{aligned} &u_d(r,t) = \sum_m a_m(t)\varphi_m(r) \\ &\varphi_m(r) = \sum_{j=1}^{N_r} k_{ejm}(c_{1jm}J_1(k_{ejm}r) + c_{2jm}Y_1(k_{ejm}r))(H(r-r_j) - H(r-r_{j+1})) \end{aligned} \tag{34}$$

$H(r)$ is the Heaviside function, $k_{e\,j\,m} = \omega_m/c_{e\,j}$ and ω_m is the mth eigen*frequency*. Substituting (32a,b) in (31) then in (25) and enforcing orthogonality of the $\{\varphi_m\}$ set yields uncoupled equations in $a_m(t)$

$$\begin{aligned} &\ddot{a}_m(t) + \omega_m^2 a_m(t) = \bar{f}_m(t) \\ &\bar{f}_m(t) = N_{sm}\ddot{f}_p(t)/N_m, \quad N_m = \int_{r_p}^{r_o} \varphi_m^2 r\,\mathrm{d}r, \quad N_{sm} = \int_{r_p}^{r_o} \varphi_m u_s r\,\mathrm{d}r \end{aligned} \tag{35}$$

Eq. (35) admits the solution

$$a_m(t) = -\frac{1}{\omega_m}\int_0^t \sin\omega_m(t-\tau)\bar{f}_m(\tau)\,\mathrm{d}\tau \tag{36}$$

4. Results

Consider a plane-strain cylinder with properties

$$\begin{aligned} &E_0 = 3.1 \times 10^9\ \mathrm{dyn/cm^2}, \quad \rho = 0.93\ \mathrm{g/cm^3}, \quad v = 0.48 \\ &r_p = 0.635\ \mathrm{cm}, \quad r_o = 7.62\ \mathrm{cm} \end{aligned} \tag{37}$$

This yields extensional and shear wave speeds c_e and c_s 1.71 and 0.34 km/s and the ratio $c_e/c_s \simeq 5$. Fig. 1 plots the resonant frequency spectrum Ω versus discrete n with radial wave number m as parameter.

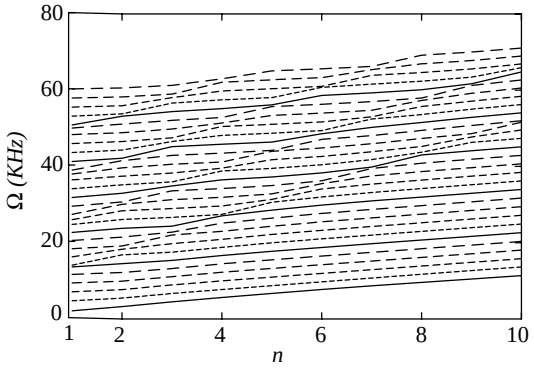

Fig. 1. Asymmetric mode frequency spectrum of homogeneous plane-strain cylinder.

Although each frequency corresponds to a discrete integer n value, the points are joined to facilitate discerning constant m lines in the explanation to follow. Lines of constant m are almost parallel with slope proportional to c_s. A constant m-line L_m changes slope and coalesces with the next constant m-line L_{m+1} without crossing it. Coalescence without crossing is necessary for uniqueness of the eigenstates. Near coalescence, L_m reverts to its original slope while L_{m+1} proceeds through similar steps to coalesce with L_{m+2} and so on. Remote from coalescence, these lines have a slope proportional to c_s and correspond to shear modes. Near coalescence, envelopes are also straight lines with slope proportional to c_e and correspond to extensional modes. Shear modes are denser than extensional modes when c_e/c_s is large as in the present case. Coupling of shear and extensional modes for $n \geqslant 1$ is what distinguishes asymmetric from axisymmetric motions.

Since the static solution is prerequisite to solving transient response, understanding the effect of θ-inhomogeneity on the static problem will help understanding its effect on transient response. The first step starts with the simple case of the static axisymmetric homogeneous cylinder with unit prescribed pressure at its inner boundary $r = r_p$. Fig. 2 plots radial distribution of displacement u_0 and stresses σ_{rr0} and $\sigma_{\theta\theta0}$. Remote from $r = r_p$, $u_0 \propto 1/r$ and $(\sigma_{rr0}, \sigma_{\theta\theta0}) \propto 1/r^2$, with magnitude equal to applied pressure p_0. As expected, σ_{rr0} is compressive and $\sigma_{\theta\theta0}$ is tensile since internal pressure expands the cylinder along the radius.

Consider the plane-strain cylinder with θ-inhomogeneity in the form of Eq. (4) including only 2 terms

$$\mu(\theta) = \mu_0(1 + 0.5\cos(2\theta)) \tag{38}$$

$\mu(\theta)$ in (38) is symmetric about $\theta = 0$ and $\theta = \pi/2$ requiring that only even n's be included in the expansion (C.8) of Appendix C. Convergence of the static solution was achieved with $m = 60$ and $n = 0$, 2, 4. Fig. 3(a1–e1) plots dependent variable along r with θ as parameter and Fig. 3(a2–e2) plots these variables along θ with r as parameter. At $\theta = 0$ where E is largest (Fig. 3(a1)), u_c decreases along r like u_0 in Fig. 2(a) with peak $u_{cmx}(r_p, 0)$ at $r = r_p$ slightly less than that of u_0. As θ increases, $u_{cmx}(r_p, \pi/4)$ diminishes to almost 1/2 $u_{cmx}(r_p, 0)$.Along θ (Fig. 3(a2)), u_c is periodic following approximately the $\cos(2\theta)$ distribution of $\mu(\theta)$. This means that along a constant r-line, the cross-section is squashed with larger curvature at $\theta = 0$ and smallest curvature at $\theta = \pi/2$. This results in flexure of the cross-section adding to $\sigma_{\theta\theta c}$ a periodic stress component that changes from compressive at $\theta = 0$ to tensile at $\theta = \pi/2$. Indeed Fig. 3(d1,d2) shows a compressive over-stress at $\theta = 0$ with magnitude $6p_0$ and a tensile over-stress with magnitude $2p_0$. The same argument applies to σ_{zzc} in Fig. 3(e1,e2). Note that in Fig. 2 σ_{zz0} is not plotted since it is small because $\sigma_{zz0} = \beta_0/(1 + \beta_0)r_p^2/\ (r_o^2 - r_p^2) \approx r_p^2/r_o^2 \ll 1$. It appears then that in the static case, θ-inhomogeneity magnifies compressive and tensile stresses because of flexure at and near the inner boundary, and raises axial stress substantially from the homogeneous case.

Consider transient response of a homogeneous plane-strain cylinder forced by a 10 μs trapezoidal pulse of unit intensity, with 1 μs rise and fall times and a 8 μs plateau. Fig. 4 plots histories of dependent variables

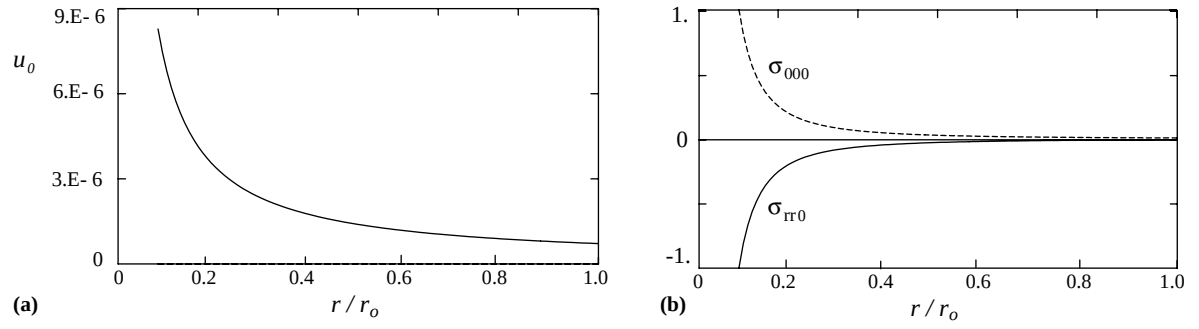

Fig. 2. Axisymmetric static variables of homogeneous plane strain cylinder.

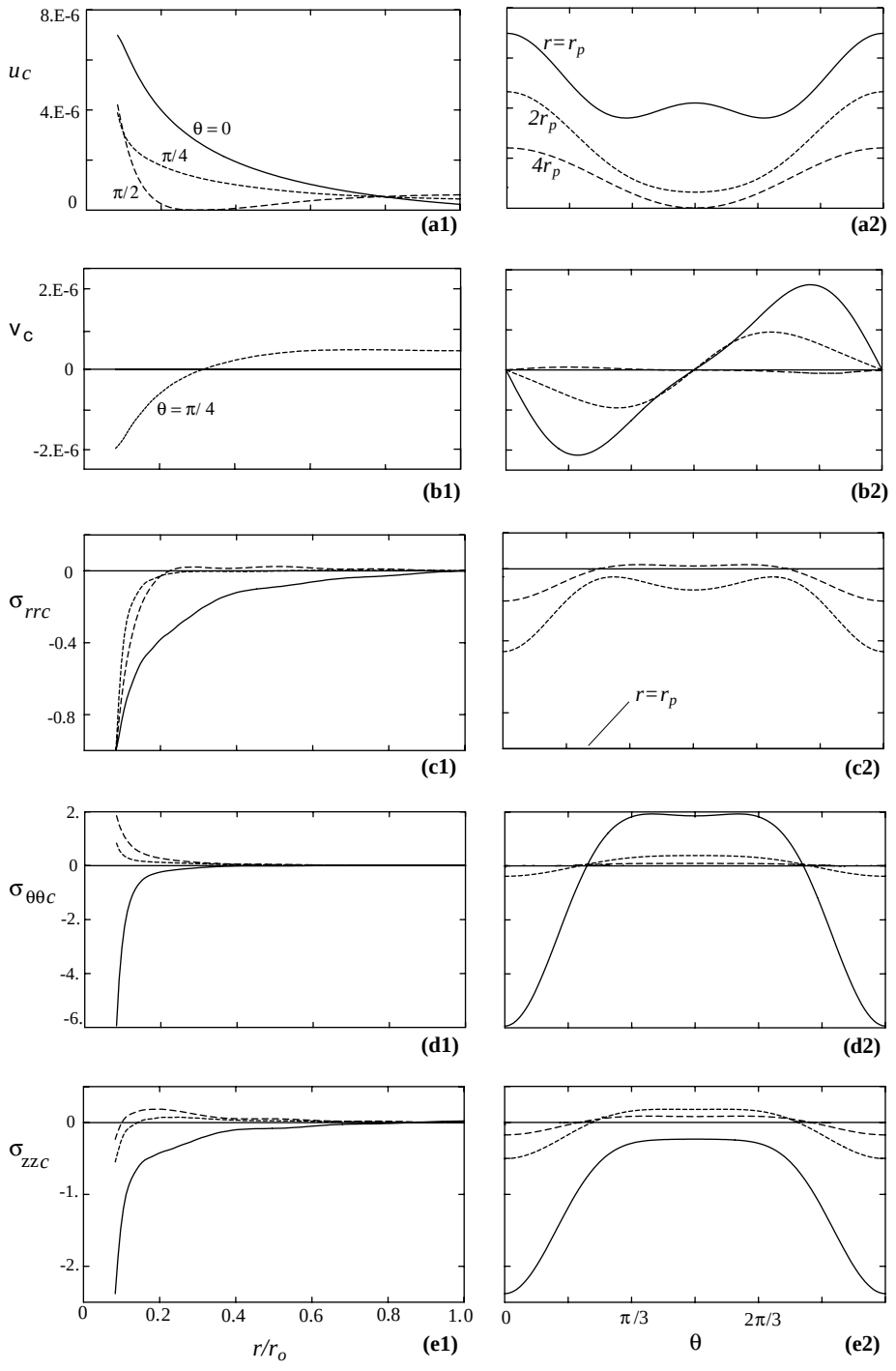

Fig. 3. Static variables of plane-strain cylinder with θ-inhomogeneity (a1)–(e1) along r, (a2)–(e2) along θ.

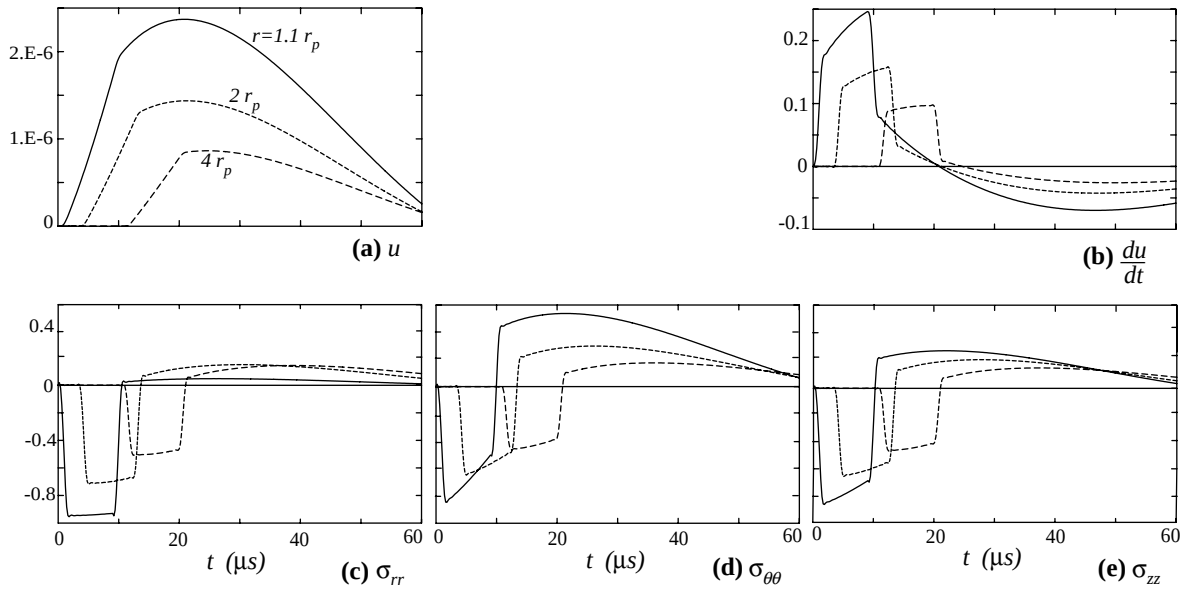

Fig. 4. Histories of homogeneous plane-strain cylinder: (a) u, (b) du/dt, (c) σ_{rr}, (d) $\sigma_{\theta\theta}$, (e) σ_{zz}.

within a 60 μs time range. Fig. 4(a) shows u histories at three different radial stations. u increases almost linearly while the forcing pulse is nonzero then drops smoothly until waves reflect from the free boundary $r = r_o$. Note the time delay in response for $r = 2r_p$ and $r = 4r_p$ equal to travel time of extensional waves to reach these stations from $r = r_p$. Fig. 4(b) plots velocity history. Velocity increases steeply with rise time that of the forcing pulse, then continues to increase at a reduced rate until the forcing pulse elapses consistent with the shape of the u history in Fig. 4(a). The smooth rise during the plateau portion of the pulse is characteristic of cylindrical symmetry as it is flat in 1-D and 2-D. σ_{rr} follows the shape of the forcing pulse closely since it must satisfy the boundary condition at $r = r_p$ (see Fig. 4(c)). However, $\sigma_{\theta\theta}$ while being tensile for all r in the static case (Fig. 2(b)), is compressive throughout the duration of the pulse then changes to tensile after the pulse elapses. An explanation is that shortly after the pulse is applied, a narrow annular region bounded by the extensional wave-front undergoes stress while the wave-front acts as a solid but moving boundary. During this time, the state of stress in this instantaneously confined annular region is almost hydrostatic where all three normal stress components are approximately equal. Release of pressure at the end of the pulse and radial motion of the wave-front reverts to the free motion when $\sigma_{\theta\theta}$ changes to tensile.

Consider transient response of the plane-strain cylinder with the θ-inhomogeneity given by (38). Fig. 5 plots histories of each dependent variable along a column for a specific θ. Three values of θ are chosen: 0, $\pi/4$, $\pi/2$. Unless specified on the ordinate of some variable, labels along a row are the same for all θ. Exceptions to this rule are when the variable at $\theta = 0$ is substantially larger than that for other values of θ. At $\theta = 0$ (Fig. 5(a1)), magnitudes of the u histories are approximately half those for the other θ's. This may seem counter intuitive as it is the opposite of the static case (Fig. 3(a1,a2)). Yet, the explanation is the same as that for the sign of $\sigma_{\theta\theta}$ in the homogeneous cylinder (Fig. 4(d)). Shortly after the pulse is applied, the wave-front confines a narrow annular region near $r = r_p$ where the state of stress is hydrostatic. Since at $\theta = 0$, modulus is 3 times larger than at $\theta = \pi/2$, and since hydrostatic displacement is inversely proportional to modulus, the result in Fig. 5(a1) is obtained. Histories of circumferential displacement v are plotted only for $\theta = \pi/4$ (Fig. 5(b2)) since $v \propto \sin(n\theta)$ vanishes at $\theta = 0$ and $\theta = \pi/2$ for $n = 2$ and $n = 4$.

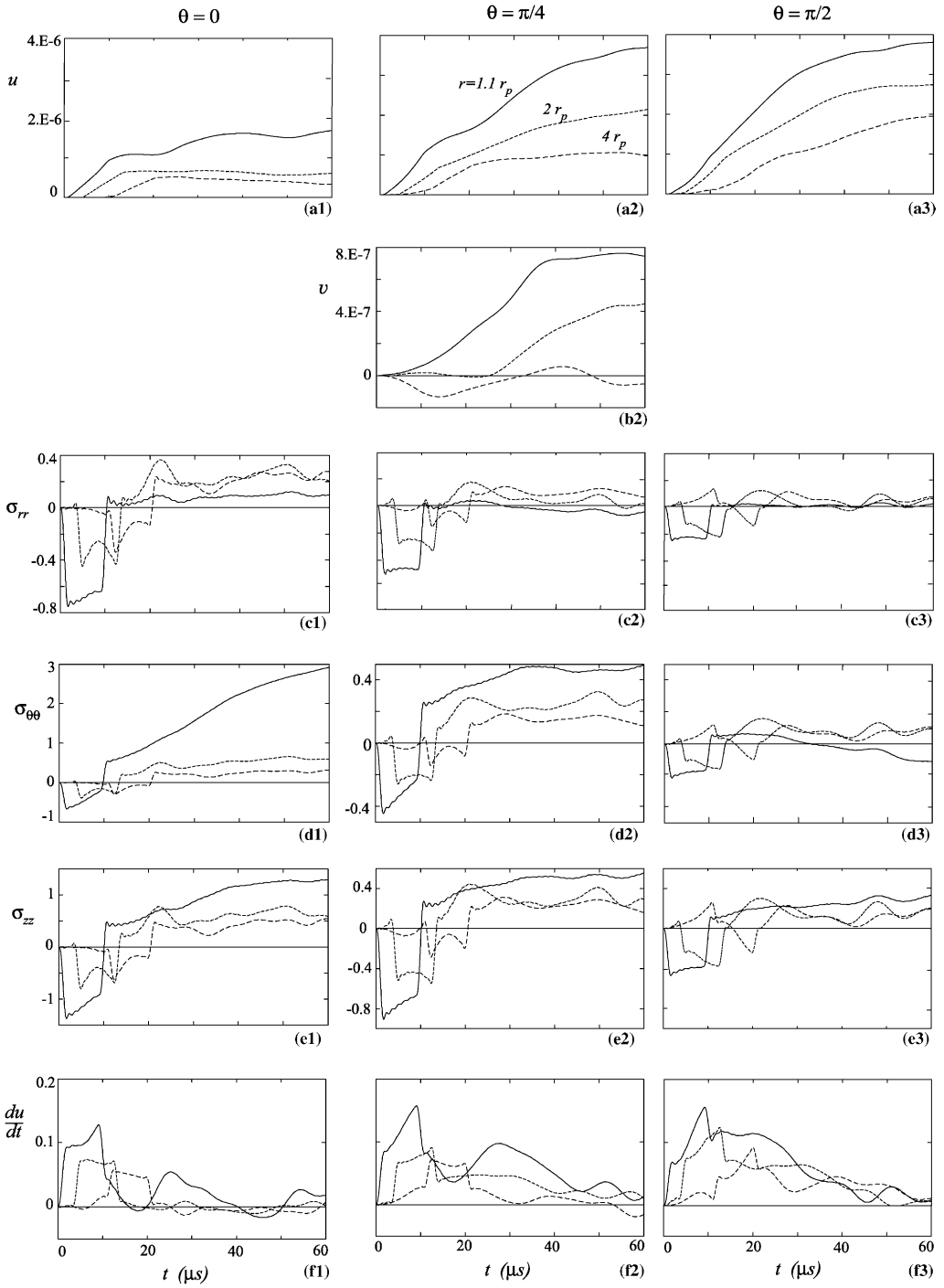

Fig. 5. Histories of plane-strain cylinder with θ-inhomogeneity (a1)–(f1) $\theta = 0$, (a2)–(f2) $\theta = \pi/4$, (a3)–(f3) $\theta = \pi/2$.

Magnitude of v is approximately 1/5 that of u for the θ shown. Also, travel time is approximately 5 times that for u in Fig. 5(a2). This implies that v propagates at the speed of shear waves c_s. Histories of σ_{rr} (Fig. 5(c1–c3)) qualitatively resemble the corresponding ones of the homogeneous cylinder (Fig. 4(c)). The difference is that magnitude of σ_{rr} reduces with modulus as evidenced by comparing Fig. 5(c1) to Fig. 5(c2,c3). Histories of $\sigma_{\theta\theta}$ at $\theta = 0$ (Fig. 5(d1)) are particularly interesting. Throughout the duration of the pulse, response is comparable to the homogeneous cylinder. After the pulse elapses, $\sigma_{\theta\theta}$ becomes tensile reaching a peak $3.5p_0$ at $t = 90$ μs. The first peak of $\sigma_{\theta\theta}$ occurs at the 1/4 period of the coupled fundamental resonance with a frequency of 2.6 kHz compared to the fundamental axisymmetric resonance of the homogeneous cylinder at 6.1 kHz. For an impulsive pressure, setting $\bar{f}_i(\tau) = \delta(\tau)$ in (23a) yields $a_i(t) \propto \sin(\omega_i t)/\omega_i$ implying that the largest amplitude of free oscillation is inversely proportional to the fundamental resonance. This explains the larger $\sigma_{\theta\theta}$ amplitude of the inhomogeneous cylinder compared the homogeneous one. Histories of σ_{zz} (Fig. 5(e1–e3)) resemble those of σ_{rr} (Fig. 5(c1–c3)) except that magnitude at $\theta = 0$ is approximately double that at $\theta = \pi/4$. Finally, velocity histories (Fig. 5(f1–f3)) follow the u histories (Fig. 5(a1–a3)) in that magnitude of velocity at $\theta = 0$ is lower than that at $\theta = \pi/4$ and at $\theta = \pi/2$.

In the case of r-inhomogeneity assume the following distribution of modulus $E(r)$

$$E(r) = E_0(1 + 0.5\sin(4\pi(r - r_p)/(r_o - r_p))) \tag{39}$$

where E_0 and all other properties are given in (37). In this way, the highest to lowest $E(r)$ ratio is 3 similar to the θ-inhomogeneity. The cylinder is divided into 45 annular constant width segments each assigned a constant $E(r_i)$ following (39) with r_i being the mean radius of the ith segment. The corresponding stepwise c_e distribution is shown in Fig. 6. The cylinder is forced by the same 10 μs trapezoidal pulse used in the case of the θ-inhomogeneity. Fig. 7(a–e) plots histories of the cylinder in the interval $0 \leqslant t \leqslant 80$ μs. Throughout the duration of the pulse, histories of the cylinder with r-inhomogeneity are almost the same as those of the homogeneous case (see Fig. 4). During this time, response is confined to a narrow ring close to $r = r_p$, where magnitude depends only on properties in this region. After the pulse elapses and the wave-front moves outward, response then differs from the homogeneous case especially after reflection from the outer boundary $r = r_o$.

It is evident from the examples above that for the same level of inhomogeneity, θ-inhomogeneity has a more pronounced effect on transient response both in shape and magnitude. The fundamental reason is that with a θ-inhomogeneity, asymmetric waves are excited that include both extensional and shear components adding to the spectrum modes with lower frequency. These modes magnify amplitude of free motion for all dependent variables.

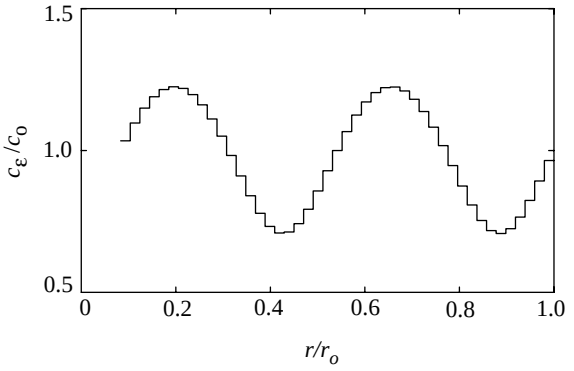

Fig. 6. Radial stepwise distribution of normalized c_ε.

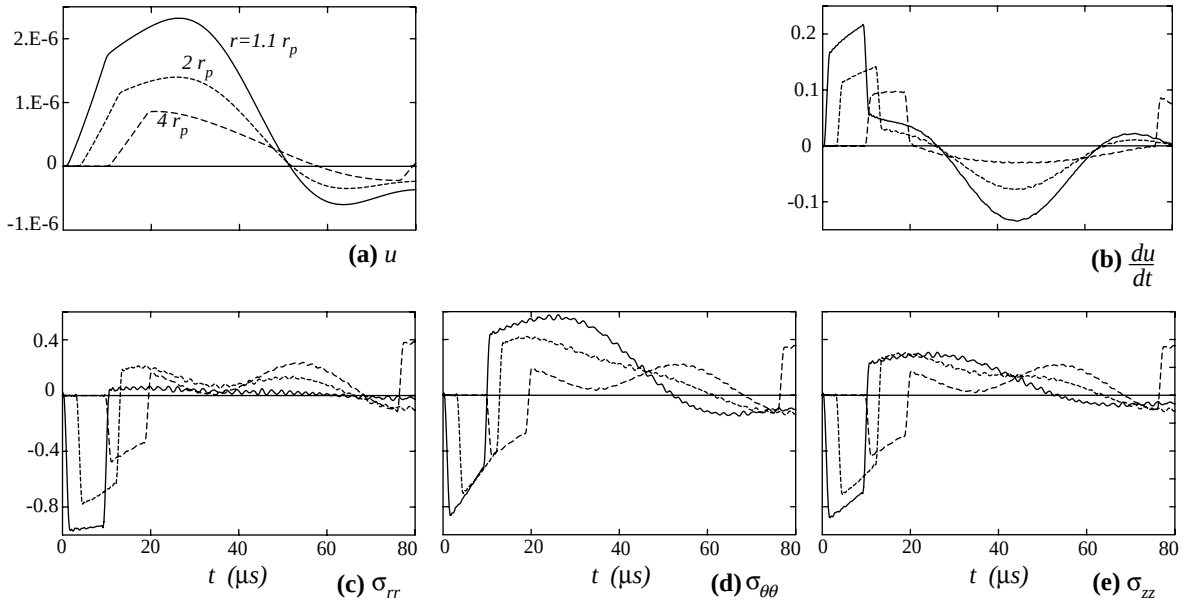

Fig. 7. Histories of plane-strain cylinder with r-inhomogeneity: (a) u, (b) du/dt, (c) σ_{rr}, (d) $\sigma_{\theta\theta}$, (e) σ_{zz}.

5. Conclusion

Transient response of a plane-strain hollow cylinder was analyzed for both θ- and r-inhomogeneity. For a θ-inhomogeneity with periodic modulation noteworthy results are

1. Dependent variables acquire a periodicity along the circumference.
2. Static $\sigma_{\theta\theta}$ and σ_{zz} are magnified at $\theta = 0$ and $r = r_p$ compared to the homogeneous case.
3. Static $\sigma_{\theta\theta}$ is modulated by a flexural components that is compressive along the axis of highest modulus and tensile along the axis of weakest modulus.
4. Asymmetric waves are induced that include extensional and shear components adding modes with lower frequencies to the spectrum. This in turn magnifies amplitude of $\sigma_{\theta\theta}$ and σ_{zz} after the forcing pulse elapses and free harmonic motion starts.

For a periodic r-inhomogeneity the principal results are

1. When the forcing pulse is acting, response resembles the homogeneous case.
2. Differences in response appear after the pulse elapse especially after reflection from the outer boundary.
3. Fixing the level of inhomogeneity, θ-inhomogeneity has a more pronounced effect on response than r-inhomogeneity because of the absence of shear waves in the latter.

Acknowledgments

This work was supported by a grant from DARPA, executed by the US Army Medical Research and Material Command/TATRC Contract# W81XWH-04-C-0084. The views, opinions and/or findings contained in this paper are those of the author and should not be construed as an official Department of the Army position, policy or decision unless so designated by other documentation.

Appendix A. Asymmetric dynamic solution of homogeneous finite cylinder

For periodic motions in time, The Navier equations of elastodynamics can be written in vector form as

$$(\lambda+\mu)\nabla(\nabla\cdot\mathbf{u})+\mu\nabla\cdot(\nabla\mathbf{u})+\rho\omega^2\mathbf{u}=\mathbf{0} \tag{A.1}$$

where λ and μ are *Lame*'s constants, ρ is density, $\mathbf{u}$ is displacement vector, and ω is radian frequency. For cylindrical coordinates (r,θ,z) where z is along the axis of revolution, $\mathbf{u}$ can be expressed in terms of three scalar potentials φ, ξ, η as follows:

$$\begin{aligned}&\mathbf{u}=\nabla\varphi+\nabla\times(\xi\mathbf{e}_z)+\nabla\times\nabla\times(\eta\mathbf{e}_z)\\&\mathbf{u}\equiv u\mathbf{e}_r+v\mathbf{e}_\theta+w\mathbf{e}_z\end{aligned} \tag{A.2}$$

where $\mathbf{e}_r$, $\mathbf{e}_\theta$, $\mathbf{e}_z$ are a unit vectors along r, θ, z. Substituting (A.2) in (A.1) then taking the divergence yields

$$\begin{aligned}&\nabla^2\varphi+k_e^2\varphi=0,\quad \nabla^2\equiv\partial_{rr}+1/r\partial_r+1/r^2\partial_{\theta\theta}+\partial_{zz}\\&k_e=\omega/c_e,\quad c_e^2=(\lambda+2\mu)/\rho\end{aligned} \tag{A.3}$$

Substituting (A.2) in (A.1) and taking the curl yields

$$\begin{aligned}&\nabla^2\xi+k_s^2\xi=0\\&\nabla^2\eta+k_s^2\eta=0\\&k_s=\omega/c_s,\quad c_s^2=\mu/\rho\end{aligned} \tag{A.4}$$

For simply-supported boundary conditions at $z=0$, l and periodicity along θ, (φ,ξ,η) can be expressed in terms of Bessel functions in r and harmonic functions in θ and z

$$\begin{aligned}&\varphi(r,\theta,z)=(c_{11}J_n(k_{re}r)+c_{21}Y_n(k_{re}r))S_m(z)C_n(\theta)\\&\xi(r,\theta,z)=(c_{12}J_n(k_{rs}r)+c_{22}Y_n(k_{rs}r))S_m(z)S_n(\theta)\\&\varphi(r,\theta,z)=(c_{13}J_n(k_{rs}r)+c_{23}Y_n(k_{rs}r))C_m(z),C_n(\theta)\end{aligned} \tag{A.5a}$$

$$\begin{aligned}&S_n(\theta)=\sin(n\theta),\quad C_n(\theta)=\cos(n\theta)\\&S_m(z)=\sin(k_{zm}z),\quad C_m(z)=\cos(k_{zm}z)\\&k_{re}^2=k_e^2-k_{zm}^2,\quad k_{rs}^2=k_s^2-k_{zm}^2,\quad k_{zm}=m\pi/l\\&m=1,2,\ldots,M,\quad n=0,1,\ldots,N\end{aligned} \tag{A.5b}$$

m is an integer axial wave number that follows from the exact solution of the separated axial dependence satisfying simply supported boundary conditions at $z=0,l$ which require that $u(r,\theta,z)=v(r,\theta,z)=\sigma_{zz}(r,\theta,z)=0$ at $z=0$, l. Similarly, n is an integer circumferential wave number that follows from the exact solution of the separated circumferential dependence satisfying continuity of dependent variable along the cylinder's circumference. Subscript m in k_{zm} will be dropped hereafter for shortness.

If D is a dependent variable, then

$$\mathsf{D}(J_n,J_{n+1};Y_n,Y_{n+1})=\mathsf{D}_1(J_n,J_{n+1})+\mathsf{D}_2(Y_n,Y_{n+1}) \tag{A.6}$$

Since D_2 has the same form as D_1 except that the primitives J_n, J_{n+1} in D_1 are replaced by Y_n, Y_{n+1} in D_2, only expressions for D_1 will be listed below for shortness. Substituting (A.5) in (A.2) produces expressions for displacements

$$\begin{aligned}u_1=\sum_n\sum_m\{&c_{11mn}k_{re}(nJ_n(k_{re}r)/(k_{re}r)-J_{n+1}(k_{re}r))+c_{12mn}nJ_n(k_{rs}r)/r\\&-c_{13mn}k_{rs}k_z(nJ_n(k_{rs}r)/(k_{rs}r)-J_{n+1}(k_{rs}r))\}S_m(z)C_n(\theta)\end{aligned} \tag{A.7a}$$

$$v_1 = \sum_n \sum_m \{-c_{11mn} n J_n(k_{re} r)/r - c_{12mn} k_{rs} (n J_n(k_{rs} r)/(k_{rs} r) - J_{n+1}(k_{rs} r)) + c_{13mn} n k_z J_n(k_{rs} r)/r\} S_m(z) S_n(\theta) \tag{A.7b}$$

$$w_1 = \sum_n \sum_m \{c_{11mn} k_z J_n(k_{re} r) + c_{13mn} k_{rs}^2 J_n(k_{rs} r)\} C_m(z) C_n(\theta) \tag{A.7c}$$

The constitutive relations are

$$\begin{aligned} &\sigma_{ii} = \lambda \Delta + 2\mu \varepsilon_{ii}, \quad ii \equiv rr,\ \theta\theta,\ zz \\ &\Delta = \varepsilon_{rr} + \varepsilon_{\theta\theta} + \varepsilon_{zz} \\ &\sigma_{ij} = \mu \varepsilon_{ij}, \quad ij \equiv r\theta,\ \theta z,\ zr \end{aligned} \tag{A.8}$$

$$\begin{aligned} &\varepsilon_{rr} = \partial_r u, \quad \varepsilon_{\theta\theta} = u/r + 1/r \partial_\theta v, \quad \varepsilon_{zz} \partial_z w \\ &\varepsilon_{r\theta} = 1/r \partial_\theta u + \partial_r v - v/r \\ &\varepsilon_{\theta z} = \partial_z v + 1/r \partial_\theta w, \quad \varepsilon_{zr} = \partial_r w + \partial_z u \end{aligned} \tag{A.9}$$

Substituting (A.7) in (A.9) then in (A.8) produces

$$\sigma_{rr1} = \mu \sum_n \sum_m \{c_{11mn}((-(\beta+2)(k_{re} r)^2 + 2(n^2 - n) - \beta(k_z r)^2) J_n(k_{re} r)/r^2 + 2k_{re} J_{n+1}(k_{re} r)/r) + 2c_{12mn}((n^2 - n) J_n(k_{rs} r)/r^2 - n k_{rs} J_{n+1}(k_{rs} r)/r) - 2c_{13mn} k_z ((n^2 - n - (k_{rs} r)^2) J_n(k_{rs} r)/r^2 + k_{rs} J_{n+1}(k_{rs} r)/r)\} S_m(z) C_n(\theta) \tag{A.10a}$$

$$\sigma_{\theta\theta 1} = \mu \sum_n \sum_m \{c_{11mn}(-(2(n^2 - n) + \beta(k_e r)^2) J_n(k_{re} r)/r^2 - 2k_{re} J_{n+1}(k_{re} r)/r) + 2c_{12mn}(-(n^2 - n) J_n(k_{rs} r)/r^2 + n k_{rs} J_{n+1}(k_{rs} r)/r) + 2c_{13mn} k_z ((n^2 - n) J_n(k_{rs} r)/r^2 + k_{rs} J_{n+1}(k_{rs} r)/r)\} S_m(z) C_n(\theta) \tag{A.10b}$$

$$\sigma_{zz1} = \mu \sum_n \sum_m \{-c_{11mn}((\beta+2) k_z^2 + \beta k_{re}^2) J_n(k_{re} r) - 2c_{13mn} k_z k_{rs}^2 J_n(k_{rs} r)\} S_m(z) C_n(\theta) \tag{A.10c}$$

$$\tau_{r\theta 1} = \mu \sum_n \sum_m \{2c_{11mn}(-(n^2 - n) J_n(k_{re} r)/r^2 + n k_{re} J_{n+1}(k_{re} r)/r) - 2c_{12mn}((n^2 - n - (k_{rs} r)^2/2) J_n(k_{rs} r)/r^2 + k_{rs} J_{n+1}(k_{rs} r)/r) + 2c_{13mn} k_z ((n^2 - n) J_n(k_{rs} r)/r^2 - n k_{rs} J_{n+1}(k_{rs} r)/r) S_m(z) S_n(\theta) \tag{A.10d}$$

$$\tau_{\theta z 1} = \mu \sum_n \sum_m \{-2c_{11mn} n k_z J_n(k_{re} r)/r - c_{12mn} k_z (n J_n(k_{rs} r)/r - k_{rs} J_{n+1}(k_{rs} r)) + c_{13mn} n (k_z^2 - k_{rs}^2) J_n(k_{rs} r)/r\} C_m(z) S_n(\theta) \tag{A.10e}$$

$$\tau_{rz1} = \mu \sum_n \sum_m \{2c_{11mn} k_z (n J_n(k_{re} r)/r - k_{re} J_{n+1}(k_{re} r)) + c_{12mn} n k_z J_n(k_{rs} r)/r + c_{13mn} (k_z^2 - k_{rs}^2)(-n J_n(k_{rs} r)/r + k_{rs} J_{n+1}(k_{rs} r))\} C_m(z) C_n(\theta) \tag{A.10f}$$

$$\begin{aligned} &S_n(\theta) = \sin(n\theta), \quad C_n(\theta) = \cos(n\theta), \quad n = 0, 1, \ldots, N \\ &k_{re} = k_e = \omega/c_e, \quad k_{rs} = k_s = \omega/c_s, \quad \beta = \lambda/\mu \end{aligned} \tag{A.10g}$$

The Bessel functions in (A.5a) through (A.10) are real when ω is greater than both shear and extensional cut-off frequencies of the mth axial mode

$$\omega \geqslant \omega_{co,e}^{(m)} = k_z c_e \;\Rightarrow\; k_e \geqslant k_z, \quad \omega \geqslant \omega_{co,s}^{(m)} = k_z c_s \;\Rightarrow\; k_s \geqslant k_z \tag{A.11}$$

Since $c_e > c_s$ then (A.5a) through (A.10) are valid when $\omega \geqslant k_z c_e$. However, if $k_z c_s < \omega < k_z c_e$ then $J_n(k_{re}r)$, $Y_n(k_{re}r)$ are replaced by $I_n(k_{re}r)$, $K_n(k_{re}r)$. Similarly, if $\omega < k_z c_s$ then $J_n(k_{rs}r)$, $Y_n(k_{rs}r)$ are replaced by $I_n(k_{rs}r)$, $K_n(k_{rs}r)$. Expressions for displacement and stress similar in form to (A.7) and (A.10) follow with appropriate changes in sign but will not be listed here for shortness.

Appendix B. Asymmetric dynamic solution of plane-strain cylinder

For the plane-strain problem, displacements and stresses are found from Appendix A when the z dependence and axial displacement w vanish. Expressions for u and v are

$$\begin{aligned} u_1 &= \sum_n \{c_{11n} k_{re}(nJ_n(k_{re}r)/(k_{re}r) - J_{n+1}(k_{re}r)) + c_{12n} nJ_n(k_{rs}r)/r\} C_n(\theta) \\ v_1 &= \sum_n \{-c_{11n} nJ_n(k_{re}r)/r - c_{12n} k_{rs}(nJ_n(k_{rs}r)/(k_{rs}r) - J_{n+1}(k_{rs}r))\} S_n(\theta) \end{aligned} \tag{B.1}$$

$$S_n(\theta) = \sin(n\theta), \quad C_n(\theta) = \cos(n\theta), \quad n = 0, 1, \ldots, N$$

$$k_{re} = k_e = \omega/c_e, \quad k_{rs} = k_s = \omega/c_s$$

Expressions for stresses σ_{rr}, $\sigma_{\theta\theta}$, σ_{zz}, $\tau_{r\theta}$ are

$$\begin{aligned} \sigma_{rr1} = \mu \sum_n \{ & c_{11n}((-(\beta+2)(k_{re}r)^2 + 2(n^2-n))J_n(k_{re}r)/r^2 + 2k_{re}J_{n+1}(k_{re}r)/r) \\ & + 2c_{12n}((n^2-n)J_n(k_{rs}r)/r^2 - nk_{rs}J_{n+1}(k_{rs}r)/r)\} C_n(\theta) \end{aligned} \tag{B.2a}$$

$$\begin{aligned} \sigma_{\theta\theta 1} = \mu \sum_n \{ & c_{11n}(-(2(n^2-n) + \beta(k_e r)^2)J_n(k_{re}r)/r^2 - 2k_{re}J_{n+1}(k_{re}r)/r) \\ & + 2c_{12n}(-(n^2-n)J_n(k_{rs}r)/r^2 + nk_{rs}J_{n+1}(k_{rs}r)/r)\} C_n(\theta) \end{aligned} \tag{B.2b}$$

$$\sigma_{zz1} = \mu \sum_n \{-2c_{11n}\beta k_{re}^2 J_n(k_{re}r)\} C_n(\theta) \tag{B.2c}$$

$$\begin{aligned} \tau_{r\theta 1} = \mu \sum_n \{ & 2c_{11n}(-(n^2-n)J_n(k_{re}r)/r^2 + nk_{re}J_{n+1}(k_{re}r)/r) - 2c_{12n}((n^2 - n - (k_{rs}r)^2/2)J_n(k_{rs}r)/r^2 \\ & + k_{rs}J_{n+1}(k_{rs}r)/r)\} S_n(\theta) \end{aligned} \tag{B.2d}$$

Appendix C. Asymmetric static solution of plane-strain cylinder

For the homogeneous cylinder with material properties (λ_0, μ_0), the static solution is obtained by solving Eq. (1a) with vanishing time dependence. The solution takes the form

$$u_s(r,\theta) = c_u r^\alpha C_n(\theta), \quad v(r,\theta) = c_v r^\alpha S_n(\theta) \tag{C.1}$$

where c_u and c_υ are constant coefficients. Substituting (C.1) in (1a) yields the equations

$$\begin{aligned}&((\lambda_0+2\mu_0)(\alpha^2-1)-\mu_0 n^2)c_u+n((\lambda_0+\mu_0)\alpha-(\lambda_0+3\mu_0))c_\upsilon=0\\&n((\lambda_0+\mu_0)\alpha+(\lambda_0+3\mu_0))c_u-((\lambda_0+2\mu_0)n^2-\mu_0(\alpha^2-1))c_\upsilon=0\end{aligned}\tag{C.2}$$

A non-trivial solution requires that the determinant of the coefficients of c_u and c_υ vanish. This yields a fourth order polynomial in α with 4 roots

$$\alpha=\pm(n\pm1)\tag{C.3}$$

The solution (C.1) then takes the form

$$u_s(r,\theta)=\sum_{n=0}\sum_{i=1}^{4}c_{u,ni}r^{\alpha_{ni}}C_n(\theta)\tag{C.4a}$$

$$\upsilon_s(r,\theta)=\sum_{n=0}\sum_{i=1}^{4}c_{\upsilon,ni}r^{\alpha_{ni}}S_n(\theta)\tag{C.4b}$$

Substituting each of the roots of (C.3) in (C.2) determines a relation between $c_{u,ni}$ and $c_{\upsilon,ni}$

$$c_{\upsilon,ni}=-\frac{(\lambda_0+2\mu_0)(\alpha_{ni}^2-1)-\mu_0 n^2)}{n((\lambda_0+\mu_0)\alpha_{ni}-(\lambda_0+3\mu_0))}c_{u,ni}\tag{C.5}$$

Substituting (C.4) into the constitutive relations 2a,2b(2) gives

$$\sigma_{rrs}(r,\theta)=\sum_{n=0}\sum_{i=1}^{4}\{c_{u,ni}(\lambda_0(\alpha_{ni}+1)+2\mu_0\alpha_{ni})+c_{\upsilon,ni},n\lambda_0\}r^{\alpha_{ni}-1}C_n(\theta)$$

$$\sigma_{\theta\theta s}(r,\theta)=\sum_{n=0}\sum_{i=1}^{4}\{c_{u,ni}(\lambda_0(\alpha_{ni}+1)+2\mu_0)+c_{\upsilon,ni}n(\lambda_0+2\mu_0)\}r^{\alpha_{ni}-1}C_n(\theta)$$

$$\sigma_{zzs}(r,\theta)=\lambda_0\sum_{n=0}\sum_{i=1}^{4}\{c_{u,ni}(\alpha_{ni}+1)+c_{\upsilon,ni}n\}r^{\alpha_{ni}-1}C_n(\theta)$$

$$\tau_{r\theta s}(r,\theta)=-\mu_0\sum_{n=0}\sum_{i=1}^{4}\{c_{u,ni}n-c_{\upsilon,ni}(\alpha_{ni}-1)\}r^{\alpha_{ni}-1}S_n(\theta)\tag{C.6}$$

Substituting (C.5) in the boundary conditions

$$\sigma_{rrs}(r_p)=\sum_{n=0}^{N_\theta}p_nC_n(\theta),\quad \sigma_{rrs}(r_o)=0\tag{C.7a}$$

$$\tau_{r\theta s}(r_p)=0,\quad \tau_{r\theta s}(r_o)=0\tag{C.7b}$$

yields N_θ uncoupled linear equations in each set of coefficients $c_{u,ni}$ and $c_{\upsilon,ni}$.

For the cylinder with θ-inhomogeneity in E given by (4), the static equations (5a,b) with vanishing time derivative are solved by the Galerkin method. A set of orthogonal trial functions is assumed each satisfying the homogeneous differential equations (3) and boundary conditions (9). Candidate functions are the

eigenfunctions of the homogeneous cylinder with $n \geqslant 0$. Since the total static solution is made of the axisymmetric static solution modified by an asymmetric part accounting for material inhomogeneity, that static solution is added to the set of trial functions. In this way, the displacement expansion takes the form

$$\begin{aligned} u_s(r,\theta) &= \sum_{n=0}\sum_{m=1} b_{mn}\varphi_{mn}C_n(\theta) + u_{s0}(r) \\ v_s(r,\theta) &= \sum_{n=1}\sum_{m=1} b_{mn}\psi_{mn}S_n(\theta) \end{aligned} \tag{C.8}$$

$\{\varphi(r),\psi(r)\}_{nm}$ are the eigenfunctions of the homogeneous problem determined by (10) satisfying the homogeneous boundary conditions (9), and $u_{s0}(r)$ is static axisymmetric radial displacement defined by (C.4a) with $n = 0$, satisfying the inhomogeneous boundary conditions (C.7a)

$$u_{s0}(r) = -p_0 r_p^2 (r/(\beta_0+1) + r_o^2/r)/(2\mu_0(r_o^2 - r_p^2)), \quad \beta_0 = \lambda_0/\mu_0 \tag{C.9}$$

Substituting (C.8) in the static equivalent of (5a,b), then multiplying (5a) by $\varphi_{mn}\cos(n\theta)$ and (5b) by $\psi_{mn}\sin(n\theta)$, integrating over the domain $r_p \leqslant r \leqslant r_o$, $0 \leqslant \theta \leqslant 2\pi$ then adding the two equations produces

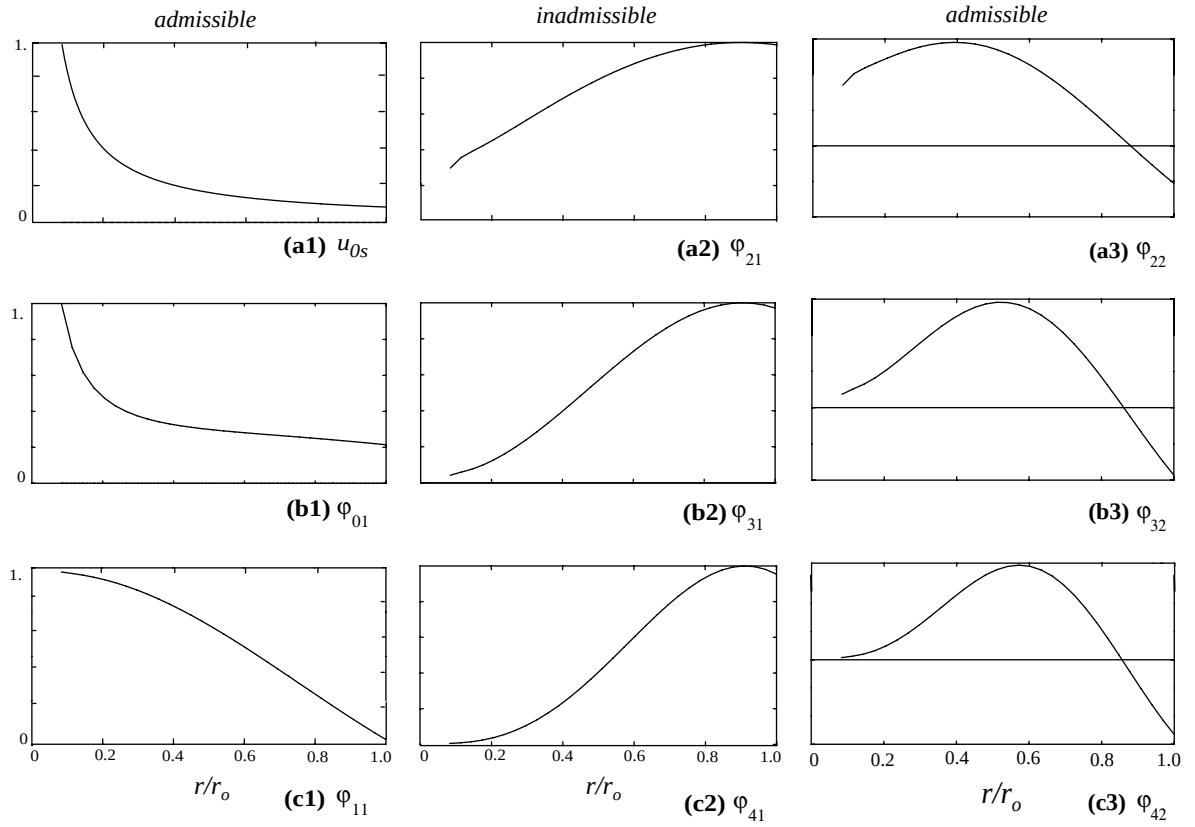

Fig. 8. Sample of low wave number admissible and inadmissible trial functions in static response: (a1) u_{0s} static $n = 0$, (a2) φ_{21} $n = 2$, $m = 1$, (a3) φ_{22} $n = 2$, $m = 2$ (b1) φ_{01} $n = 0$, $m = 1$ (b2) φ_{31} $n = 3$, $m = 1$, (b3) φ_{32} $n = 3$, $m = 2$ (c1) φ_{11} $n = 1$, $m = 1$, (c2) φ_{41} $n = 4$, $m = 1$, (c3) φ_{42} $n = 4$, $m = 2$.

$$\rho\sum_{k=0}\sum_{j=1}[\Theta^{(1)}_{nk}R^{(1)}_{mn,jk}+\Theta^{(2)}_{nk}R^{(2)}_{mn,jk}]\omega^2_{jk}b_{jk}$$
$$+\mu_0\sum_{k=0}\sum_{j=1}[\Theta^{(3)}_{nk}R^{(3)}_{mn,jk}+\Theta^{(4)}_{nk}R^{(4)}_{mn,jk}]b_{jk}=-p_0\delta_{n0}\Theta^{(4)}_{n0}R^{(0)}_{mn} \tag{C.10}$$
$$R^{(0)}_{mn}=-r_p^2/(r_o^2-r_p^2)\int_{r_p}^{r_o}\psi_{mn}(1+(r_o/r)^2)\,\mathrm{d}r$$

All other quantities in (C.10) are defined in (15b,c). The linear simultaneous equations (C.10) determine the coefficients b_{jk}.

Since the functions $\{\varphi(r),\psi(r)\}_{nm}$ are only trial functions and not solutions of the static equations, not all functions are physically admissible. In fact, the lowest mode $m=1$ for $n\geqslant 2$ is dropped for reasons to follow. Fig. 8(a1) plots normalized $u_{s0}(r)$ which varies exponentially with r. Fig. 8(b1) and (c1) plot $\varphi_{01}(r)$ and $\varphi_{11}(r)$ which follow the same qualitative behavior. For modes $\varphi_{21}(r)$, $\varphi_{31}(r)$, $\varphi_{41}(r)$ etc., this trend changes as shown in Fig. 8(a2,b2,c2) as these functions increase with r. These shapes although consistent with extensional dynamic resonances, are inconsistent with static deformation from pressure at the inner boundary as shown in Fig. 8(a1). Functions with higher wave number as $\varphi_{22}(r)$, $\varphi_{32}(r)$, $\varphi_{42}(r)$ etc. (Fig. 8(a3,b3,c3)) are all admissible. It then follows that for $n\geqslant 2$ extensional modes with $m=1$ are inadmissible trial functions excluded in the expansion (C.8).

References

Armenakas, A., 1967. Propagation of harmonic waves in composite circular cylindrical shells I: Theoretical investigation. American Institute of Aeronautics and Astronautics Journal 5, 740–744.

Armenakas, A., Keck, H., 1970. Harmonic non-axisymmetric waves with short wave lengths propagating in composite rods. Journal of the Acoustical Society of America 48, 1160–1169.

Baltrukonis, J., 1960. Free transverse vibrations of a solid mass in an infinitely long rigid circular cylindrical tank. ASME Journal of Applied Mechanics 27, 663–668.

Bird, J., Hart, R., McClure, F., 1960. Vibration of thick-walled hollow cylinders: exact numerical solutions. Journal of the Acoustical Society of America 32, 1403–1412.

El-Raheb, M., 2004. Wave propagation in a hollow cylinder due to prescribed velocity at the boundary. International Journal of Solids & Structures 41 (18–19), 5051–5069.

El-Raheb, M., Wagner, P., 1989. Wave propagation in a thin cylinder that includes point masses. Journal of the Acoustical Society of America 85, 759–767.

Gazis, D., 1958. Exact analysis of the plane-strain vibration of thick-walled hollow cylinders. Journal of the Acoustical Society of America 30, 786–794.

Heyliger, P., Jilania, A., 1992. The free vibration of inhomogeneous elastic cylinders and spheres. International Journal of Solids and Structures 29, 2689–2708.

Keck, H., Armenakas, A., 1971. Wave propagation in transversely isotropic layered cylinders. Journal of Engineering Mechanics 97, 541–558.

Reuter, R., 1969. Dispersion of flexural waves in circular bimaterial cylinders—theoretical treatment. Journal of the Acoustical Society of America 46, 643–648.

Steinberg, L., 1995. Inverse spectral problems for inhomogeneous elastic cylinders. Journal of Elasticity 38, 133–151.

Whittier, J., Jones, J., 1967. Axially symmetric wave propagation in a two-layered cylinder. International Journal of Solids and Structures 3, 657–675.

Yin, X., Yue, Z., 2002. Transient plane-strain response of multilayered elastic cylinders to axisymmetric impulse. ASME Journal of Applied Mechanics 69, 825–835.